

Long-term trends in nitrogen oxides concentrations and on-road vehicle emission factors in Copenhagen, London and Stockholm

Krecl, Patricia; Harrison, Roy M.; Johansson, Christer; Targino, Admir Créso; Beddows, David C.; Ellermann, Thomas; Lara, Camila; Ketzel, Matthias

DOI:

[10.1016/j.envpol.2021.118105](https://doi.org/10.1016/j.envpol.2021.118105)

License:

Creative Commons: Attribution-NonCommercial-NoDerivs (CC BY-NC-ND)

Document Version

Peer reviewed version

Citation for published version (Harvard):

Krecl, P, Harrison, RM, Johansson, C, Targino, AC, Beddows, DC, Ellermann, T, Lara, C & Ketzel, M 2021, 'Long-term trends in nitrogen oxides concentrations and on-road vehicle emission factors in Copenhagen, London and Stockholm', *Environmental Pollution*, vol. 290, 118105. <https://doi.org/10.1016/j.envpol.2021.118105>

[Link to publication on Research at Birmingham portal](#)

General rights

Unless a licence is specified above, all rights (including copyright and moral rights) in this document are retained by the authors and/or the copyright holders. The express permission of the copyright holder must be obtained for any use of this material other than for purposes permitted by law.

- Users may freely distribute the URL that is used to identify this publication.
- Users may download and/or print one copy of the publication from the University of Birmingham research portal for the purpose of private study or non-commercial research.
- User may use extracts from the document in line with the concept of 'fair dealing' under the Copyright, Designs and Patents Act 1988 (?)
- Users may not further distribute the material nor use it for the purposes of commercial gain.

Where a licence is displayed above, please note the terms and conditions of the licence govern your use of this document.

When citing, please reference the published version.

Take down policy

While the University of Birmingham exercises care and attention in making items available there are rare occasions when an item has been uploaded in error or has been deemed to be commercially or otherwise sensitive.

If you believe that this is the case for this document, please contact UBIRA@lists.bham.ac.uk providing details and we will remove access to the work immediately and investigate.

1 **Long-term trends in nitrogen oxides concentrations and on-road vehicle emission factors in**
2 **Copenhagen, London and Stockholm**

3

4 Patricia Krecl^{a,*}, Roy M. Harrison^{b,c}, Christer Johansson^d, Admir C. Targino^a, David C. Beddows^b,
5 Thomas Ellermann^e, Camila Lara^a, and Matthias Ketzel^{e,f}

6

7 ^aGraduate Program in Environmental Engineering, Federal University of Technology, Av. Pioneiros
8 3131, 86036-370, Londrina, PR, Brazil

9 ^bSchool of Geography, Earth and Environmental Sciences, University of Birmingham, Edgbaston,
10 Birmingham, B15 2TT, United Kingdom

11 ^cDepartment of Environmental Sciences / Center of Excellence in Environmental Studies, King
12 Abdulaziz University, PO Box 80203, Jeddah, 21589, Saudi Arabia

13 ^dDepartment of Environmental Science, Stockholm University, Svante Arrhenius väg 8, 106 91,
14 Stockholm, Sweden

15 ^eDepartment of Environmental Science, Aarhus University, Frederiksborgvej 399, DK-4000, Roskilde,
16 Denmark

17 ^fGlobal Centre for Clean Air Research (GCARE), University of Surrey, Guildford GU2 7XH, United
18 Kingdom

19

20

21

22 *Corresponding author:

23 E-mail: patriciak@utfpr.edu.br

24 **Abstract**

25 Road transport is the main anthropogenic source of NO_x in Europe, affecting human health and
26 ecosystems. Thus, mitigation policies have been implemented to reduce on-road vehicle emissions,
27 particularly through the Euro standard limits. To evaluate the effectiveness of these policies, we
28 calculated NO₂ and NO_x concentration trends using air quality and meteorological measurements
29 conducted in three European cities over 26 years. These data were also employed to estimate the trends
30 in NO_x emission factors (EF_{NO_x}, based on inverse dispersion modeling) and NO₂:NO_x emission ratios
31 for the vehicle fleets under real-world driving conditions. In the period 1998-2017, Copenhagen and
32 Stockholm showed large reductions in both the urban background NO_x concentrations (-2.1 and -2.6 %
33 yr⁻¹, respectively) and EF_{NO_x} at curbside sites (68 and 43%, respectively), proving the success of the Euro
34 standards in diminishing NO_x emissions. London presented a modest decrease in urban background NO_x
35 concentrations (-1.3% yr⁻¹), while EF_{NO_x} remained rather constant at the curbside site (Marylebone Road)
36 due to the increase in public bus traffic. NO₂ primary emissions –that are not regulated– increased until
37 2008-2010, which also reflected in the ambient concentrations. This increase was associated with a strong
38 dieselization process and the introduction of new after-treatment technologies that targeted the emission
39 reduction of other species (e.g., greenhouse gases or particulate matter). Thus, while regulations on
40 ambient concentrations of specific species have positive effects on human health, the overall outcomes
41 should be considered before widely adopting them. Emission inventories for the on-road transportation
42 sector should include EF_{NO_x} derived from real-world measurements, particularly in urban settings.

43

44

45

46 **Key words:** NO_x; air quality in Europe; OSPM model; road transport; dieselization.

47 **1. Introduction**

48 Road transport is the main anthropogenic source of nitrogen oxides (NO_x) on a global scale (23% in
49 2017, McDuffie et al., 2020) and across Europe (39% in 2017, EEA, 2019). In traffic environments, NO_x
50 consists mainly of nitric oxide (NO) and nitrogen dioxide (NO₂), with the latter associated with a series
51 of deleterious health effects (Nathan and Cunningham-Bussel, 2013; Brown, 2015; Atkinson et al., 2018).
52 Moreover, NO_x affects human health indirectly –through the production of surface ozone (O₃) (Monks
53 et al., 2015) and secondary inorganic aerosol (Fuzzi et al., 2015)– and impacts the environment –through
54 eutrophication and acidification of sensitive ecosystems (Peel et al., 2013).

55 European countries, in particular those in the northwest, have pioneered strategies to tackle
56 environmental issues, with prominent roles in the international community (Lieverink et al., 2009;
57 Grennfelt et al., 2020). In that context, air pollution has been a major political concern in Europe since
58 the late 1970s, leading to the development of ambient air quality standards and control of the major
59 emissions sources (Crippa et al., 2016). In the case of road transport, new vehicles have had to meet
60 increasingly stringent emission limits since the early 1990s, established by the so-called ‘Euro emission
61 standards’ (European Commission, 2021). These standards are based on emission factors (EF) measured
62 in laboratories under controlled conditions following regulatory driving cycles.

63 However, field studies revealed that the EF simulated with traffic emission models (COMputer
64 Programme to calculate Emissions from Road Transport COPERT, and Handbook Emission Factors for
65 Road Transport HBEFA), and validated with laboratory-based EF, largely underestimated the real
66 exhaust emissions (Carslaw et al., 2011; Carslaw and Rhys-Tyler, 2013; Krecl et al., 2017). Because
67 laboratory-based EF are used to compile the official national inventories for the road transport sector, it
68 is of utmost importance to conduct real-world EF measurements to identify mismatches in the emission
69 models (Franco et al., 2013). In light of this, the European Union through the Real Driving Emissions

70 mandates that laboratory tests be complemented with real driving condition tests for new passenger cars
71 (PC) and light-commercial vehicles (LCV) since September 2019 (European Commission, 2021). On the
72 other hand, to assess how EF has responded to policies on emission reduction and its long-term trend,
73 we need to consider approaches based on continuous measurements over a long period. In that context,
74 extended datasets of ambient air pollutant concentrations at roadside sites available in several European
75 cities can be used.

76 In the case of nitrogen species, only NO_x emissions are regulated for on-road vehicles in Europe, despite
77 NO₂ being also directly emitted by vehicle exhausts (Carslaw et al., 2011). The NO₂:NO_x emission ratios
78 largely increased in Europe in the period 1995-2010 (Grange et al., 2017), and the annual air quality
79 standard for NO₂ was still exceeded at 10% of the European stations (329 out of 3260), mainly near roads
80 (European Environmental Agency, 2019). This is particularly worrying since roadside stations are
81 located in densely populated areas where population exposure can be large.

82 Based on unique long-term datasets, this study analyzed the trends of NO₂ and NO_x concentrations at
83 three curbside sites in three European cities: Copenhagen, London and Stockholm. Then, EF_{NO_x} for the
84 vehicle fleet were determined based on the street increment of the NO_x concentrations and inverse
85 modeling techniques. The NO₂:NO_x vehicles emission ratios were estimated using their respective
86 ambient concentrations as proxies. We compare our EF_{NO_x} values for the mixed fleet with EF extracted
87 from databases and remote sensing studies. Finally, the temporal evolutions of EF_{NO_x} and primary NO₂
88 emissions are discussed in relation to regional and local policies applied to mitigate the road transport
89 emissions.

90

91

92

93 **2. Methods**

94 **2.1 Sampling sites and instrumentation**

95 We selected paired street canyon and urban background sites in Copenhagen, London and Stockholm,
96 where long-term hourly NO_x (NO+NO₂), O₃ and traffic measurements were available. Another criterion
97 was the availability of meteorological data at stations representative of winds above the corresponding
98 street canyons (Table 1, and Supplementary Material). NO_x and O₃ concentrations were measured using
99 chemiluminescence and ultraviolet photometry analyzers, respectively, complying with European
100 reference methods (EN14211, 2012; EN14625, 2012). Note that the measurements conducted at the air
101 pollution and meteorological sites are subject to rigorous quality assurance procedures since they belong
102 to national networks.

103 Hourly traffic data consisted of traffic volume (TR) and vehicle speed (VS). Traffic measurements were
104 continuously recorded on Hornsgatan St. (Stockholm) (Krecl et al., 2017) and Marylebone Road
105 (London) (Harrison et al., 2011) by using loop-profilers embedded in the surface. In the case of Jagtvej
106 St. (Copenhagen), pre-defined traffic data profiles provided by the Danish Operational Street Pollution
107 model (OSPM) were scaled up by the annual average daily traffic (AADT) and mean vehicle speed as
108 described in the Supplementary Material, together with details of traffic data validation.

109

110 **2.2 Data processing**

111 **2.2.1 Trend analysis of atmospheric concentrations**

112 Trends in air pollutant concentrations can be driven by changes in meteorological conditions, emissions,
113 atmospheric chemistry or the built environment (Grange and Carslaw, 2019; Malley et al., 2018). When
114 trend analysis is conducted for assessing the success of certain air quality management strategies, the
115 influence of the weather conditions on ambient concentrations should be removed. Thus, we applied the

116 *rmweather* R package (version 0.1.51; Grange and Carslaw, 2019) on hourly concentrations measured at
117 all sites to remove this influence. The package builds Random Forest models that predict hourly NO_x (or
118 NO₂) concentrations based on several independent variables, and then estimates the meteorologically
119 normalized series. We used the following explanatory variables: Unix date (number of seconds elapsed
120 since Jan. 1, 1970) representing the trend term, Julian day (day of the year) as the seasonal trend, day of
121 the week, hour of the day, and meteorological variables (Table 1). The importance of the predictor
122 variables on the air pollutant concentrations was also assessed with the *rmweather* package. Further
123 details on the model development and normalization technique are given in the Supplementary Material.
124 The normalized hourly ambient concentrations were aggregated to mean monthly values, which were
125 subsequently used to estimate linear trends by the non-parametric Theil-Sen method (Snell et al., 1996)
126 for each pollutant and site over the common period (1998-2017). The Theil-Sen trend is a median slope
127 trend line resistant to outliers. It was calculated with the *TheilSen* function available in the *openair* R
128 package (Carslaw and Ropkins, 2012), which also computed the confidence intervals at 95% and *p*-
129 values by bootstrap resampling.

130

131 **2.2.2 Calculation of NO₂:NO_x emission ratios**

132 We estimated the NO₂:NO_x vehicle emission ratios by filtering ambient concentrations of NO₂ and NO_x
133 measured at curbside sites following Grange et al. (2017). This technique isolates the primary NO₂
134 component by selecting measurements conducted in periods when the production of NO₂ via the NO+O₃
135 reaction is negligible. Thus, we chose only NO₂ and NO_x concentrations corresponding to traffic-
136 dominated periods (06:00-18:00 on weekdays), with low O₃ background concentrations. An O₃ threshold
137 of 10 µg m⁻³ was found appropriate to minimize the NO₂ secondary production and still have enough
138 measurements for the emission ratio calculation (more details are provided in the Supplementary
139 Material). For each curbside site and year combination, we calculated the slope of the robust linear

140 regression between the filtered NO_x and NO₂ atmospheric concentrations, which is a proxy of the
141 primary NO₂:NO_x emission ratio.

142

143 **2.2.3 Determination of EF_{NO_x}**

144 For each street canyon and year, hourly EF_{NO_x} [g veh⁻¹ m⁻¹] were determined for the mixed fleet as
145 follows (Ketznel et al., 2003; Krecl et al., 2018):

146

$$147 \quad EF_{NO_x} = \frac{\Delta NO_x(t) D(t)}{TR(t)}, \quad (1)$$

148

149 where ΔNO_x [g m⁻³] is the measured increment concentration (curbside minus urban background
150 concentrations) due to the emissions of vehicles driving on that street, TR [veh s⁻¹] is the total traffic
151 volume on that street, *D* [m² s⁻¹] is the dilution rate and *t* is the time [s]. The dilution rate depends on
152 wind conditions, traffic characteristics (TR and VS) and street canyon geometry, and was computed by
153 inverse dispersion modeling using the OSPM (Berkowicz, 2000). Details on the inverse modeling
154 technique can be found elsewhere (Palmgren et al., 1999; Ketznel et al., 2003).

155 The OSPM has been extensively tested (Kakosimos et al., 2010) and successfully simulates the NO_x
156 concentrations at regular street canyons, such as Jagtvej and Hornsgatan (Ottosen et al., 2015). However,
157 an initial screening of our OSPM results revealed abnormally high *D* values (> 24 m² s⁻¹) at Marylebone
158 Road site associated with northerly winds with WS > 2.0 m s⁻¹, which we attributed to the more complex
159 street canyon geometry. This wind condition was not very frequent (12%), but may lead to the
160 overestimation of both the dilution and the mean EF_{NO_x} values if it prevails for certain hours. Thus, these
161 occurrences were excluded from further analysis.

162 Only hourly EF_{NO_x} values for the period 07:00-23:00 on weekdays were considered for the analysis
163 because (i) the fleet composition is rather similar between weekdays, and (ii) it avoids the large
164 uncertainties in EF_{NO_x} calculations associated with the small street increments and low TR, typically
165 observed in the early hours on weekdays (Krecl et al., 2018). Then, mean annual values were calculated
166 for the years displayed in Table 1. Further details on EF_{NO_x} calculations and OSPM model setup are given
167 in the Supplementary Material.

168

169 **2.2.4 Validation with other databases**

170 The EF_{NO_x} computed by inverse modeling (Eq. 1) was compared with $EF_{NO_x_w}$ calculated by aggregating
171 $EF_{NO_x_{i,j,k}}$ per vehicle category and weighted according to each category share n within the fleet, as
172 follows:

$$173 \quad EF_{NO_x_w} = \sum_{i,j,k} EF_{NO_x_{i,j,k}} \cdot n_{i,j,k}, \quad (2)$$

174

175 where the category is a combination of vehicle class i , fuel j and Euro standard stage k .

176 $EF_{NO_x_{i,j,k}}$ were extracted from three sources: (i) the European Monitoring and Evaluation Program
177 (EMEP) guidebook (EMEP/EEA, 2019), (ii) HBEFA V.3.3 handbook processed for typical site-specific
178 traffic conditions by Burman et al. (2019), and (iii) remote sensing studies conducted under urban driving
179 conditions in Europe (UK: Carslaw et al., 2011; Carslaw and Rhys-Tyler, 2013; Carslaw et al., 2019;
180 Ghaffarpasand et al., 2020, and Sweden: Liu et al., 2019; Zhou et al., 2020) (Table 2). We used the
181 HBEFA EF_{NO_x} for ethanol and biogas since the other two sources do not include these fuels.

182 Individual EF_{NO_x} largely depends on the vehicle category, and the vehicle category share at national and
183 municipal levels can largely differ from the typical share of the actual fleet driving on the canyon street

184 for the same year (Burman et al., 2019). Thus, we profited from the detailed in situ surveys of the vehicle
185 fleet on Hornsgatan St. for the years 2009 and 2017 to validate our EF_{NOx} against the EMEP, HBEFA
186 and remote sensing estimates. These surveys analyzed automatic number plate recordings of four million
187 vehicles, and subsequent inquiry of vehicle information from the city municipality provided detailed
188 composition of the fleet in terms of vehicle class, fuel and Euro standard stage (Burman et al., 2019).

189

190 **3. Results and Discussion**

191 **3.1 Trends in ambient concentrations**

192 The most polluted street canyon was Marylebone Road (mean of NO_x and NO_2 in 2017: 286.3 and 83.9
193 $\mu g\ m^{-3}$), followed by Hornsgatan (79.9 and 35.3 $\mu g\ m^{-3}$) and Jagtvej (55.2 and 27.5 $\mu g\ m^{-3}$). The urban
194 background air was cleanest in Stockholm (mean of NO_x and NO_2 in 2017: 13.3 and 10.7 $\mu g\ m^{-3}$)
195 followed by Copenhagen (18.4 and 15.3 $\mu g\ m^{-3}$) and London (50.4 and 32.3 $\mu g\ m^{-3}$).

196 Figure 1 shows the monthly mean NO_x and NO_2 concentrations measured at the street canyon and urban
197 background sites in Copenhagen (1994-2017), London (1998-2017) and Stockholm (1992-2017),
198 together with the street increments of NO_x and NO_2 (ΔNO_x and ΔNO_2 , respectively) and the normalized
199 concentrations. Note that the mean NO_2 annual limit of the EU air quality directive (40 $\mu g\ m^{-3}$) was
200 exceeded every year at the street canyon sites in Copenhagen (1994-2009), London (1998-2017) and
201 Stockholm (1992-2016), and the urban background site in London (1998-2003). The meteorologically
202 normalized series show a decreasing trend in NO_x , ΔNO_x and (to a lesser extent) NO_2 in Stockholm and
203 Copenhagen over the years, but London presented either modest improvements or increase in
204 concentrations at Marylebone Road (Figs. 1a-f). Over the period 1998-2017, Copenhagen and Stockholm
205 showed similar patterns in concentration reductions: (i) NO_x decreased more at curbside (55-60%) than
206 at urban background sites (41-52%), and (ii) NO_2 reductions were smaller than NO_x , and declined more
207 at urban background (35-46%) than at street canyon sites (27-35%). London exhibited a different

208 behavior, with the largest NO_x reduction recorded at the urban background site (36%), and no reductions
209 in NO₂ concentrations at the curbside site (Figs. 1b,e).

210 Although road transport dominates the total NO_x emissions in Europe (EEA, 2019), other local and non-
211 local sources might have contributed to ambient NO_x concentrations at specific sites. Hence, by
212 calculating the NO_x increment at the street canyon sites the non-local contributions are filtered out,
213 leaving only the traffic-related contributions from vehicles driving on that street. Street increments for
214 NO₂ and NO_x were higher for London compared to Stockholm and Copenhagen (Figs. 1g-i), which is
215 consistent with the ADDT values recorded at the canyon streets in the period 1998-2017: 78300, 27500
216 and 18900 respectively.

217 In general, the monthly mean concentrations at all sites showed a sawtooth pattern due to
218 meteorologically driven effects on atmospheric mixing and transport and temperature-driven effects on
219 emissions, which were removed after normalization (Fig. 1, orange lines). The analysis of the importance
220 of the explanatory variables of the Random Forest models revealed that the nitrogen oxide concentrations
221 within the street canyons were largely influenced by rooftop-level wind (WD and WS, Fig. S2a,
222 Supplementary Material). This result agrees with Krecl et al. (2015), who reported that recirculation
223 patterns governed the air pollution concentrations within Hornsgatan street canyon (Fig. S2a,
224 Supplementary Material). For example, the site-dependent Random Forest model run in our study was
225 able to capture the recirculation pattern at that site. The meteorologically normalized concentrations
226 showed non-linear associations with WS, with dilution increasing with WS (e.g., Fig. S2b,d,
227 Supplementary Material). The main predictor for the urban background sites was WS, with high NO_x
228 concentrations associated with low WS, as also reported by Krecl et al. (2011), while WD had negligible
229 influence. This confirms that the sites can be taken as representative of urban background environment.
230 Kamińska (2019) and Laña et al. (2016) found similar results at other European sites.

231 In general, seasonal trends played a modest role on NO_x concentrations, with lower NO_x values observed
232 in summertime. This is most likely due to improved dispersion and reduced emissions, since summer
233 presents lower traffic volume (long holidays) and higher ambient temperatures might decrease NO_x
234 emissions for the diesel fleet (Grange et al., 2019).

235 The trend analysis is very sensitive to the chosen period, as reported by several studies (Grange and
236 Carslaw, 2019; Olstrup et al., 2018). Hence, we focused on the overlapping period 1998-2017 to avoid
237 the influence of site-specific conditions outside these years. Overall, there was a significant downward
238 trend in concentrations (Fig. 2), with NO_x decreasing faster than NO₂ in the three cities. At the curbside
239 sites, this pattern is explained by the higher NO₂:NO_x emission ratios due to the introduction of some
240 exhaust treatments for diesel vehicles (that convert NO to NO₂) and the accelerated penetration of diesel
241 PC (Grange et al., 2017). At urban background sites, the NO₂ concentrations are mainly controlled by
242 the photochemical conversion of locally emitted NO to NO₂ rather than direct NO₂ emissions (Keuken
243 et al., 2009; Anttila and Tuovinen, 2010). In urban atmospheres highly impacted by NO_x emissions, a
244 reduction in NO concentrations reduces the consumption of O₃ by titration (Monks et al., 2015) and,
245 specifically for Europe, the regional background O₃ has been increasing (0.20–0.59 μg m⁻³ yr⁻¹ for the
246 annual mean in 1995-2014, Yan et al., 2018). As a consequence, more O₃ is available to oxidize NO to
247 NO₂, causing a steeper downward trend of NO concentrations than NO₂ at the urban background sites.

248 To facilitate the comparison of the concentration trends among sites with different pollution levels,
249 changes were also expressed as percentage of variation per year over the period 1998-2017 (Fig. 2). The
250 reductions in NO_x concentrations in the urban background atmosphere were comparable in Copenhagen
251 and Stockholm (-2.1 and -2.6 % yr⁻¹, respectively). In Denmark, the reduction in NO_x emissions is due
252 to the increasing use of catalysts in vehicles, and installation of low-NO_x burners and denitrifying units
253 in power plants and district heating plants (Nielsen et al., 2019). In Sweden, the total decline in NO_x
254 emissions is linked to more stringent road transport emission standards, increased use of district heating

255 and introduction of a NO_x fee in 1992 for reducing industrial emissions (Swedish Environmental
256 Protection Agency, 2020). Particularly, the former might be more relevant for Stockholm where road
257 traffic is the dominant NO_x source (Johansson et al., 2008). Note that changes in the urban atmosphere
258 can be also affected by variations in the regional concentrations since they have non-negligible
259 contributions (Ellermann et al., 2017; Krecl et al., 2011). The reduction in NO_x concentrations in the
260 urban background atmosphere of London was modest (-1.3 % yr⁻¹) compared to the other two cities.

261 Figure 2 also shows that the negative trends of the NO_x street increments in Copenhagen and Stockholm
262 were even larger (-2.6 and -3.0 % yr⁻¹, respectively) than at the urban background sites. These large drops
263 were attributed to variations in the traffic emissions over time, since neither the street canyons nor the
264 adjacent areas underwent any changes in their configuration, and concentrations were already
265 meteorologically normalized. In Denmark, the largest source of NO_x emissions is road transport (30%
266 in 2017), with a 65% decrease in the period 1998-2017 (mean of -3.2 % yr⁻¹) (Nielsen et al., 2019). Based
267 on the emission inventories for Sweden in 1998 and 2017 (SCB, 2021), road traffic emissions were the
268 main NO_x sources and decreased 48.5% over the 20-year period, which corresponds to -2.4 % yr⁻¹. Thus,
269 this national reduction in traffic emissions is in the same order of the reduction in concentrations found
270 at the street canyon (-3.0% yr⁻¹). In the case of London, the main emission source for NO_x was road
271 transport (49%) in the year 2016 (Transport for London, 2016). Road transport also dominates the NO_x
272 emissions at national level in the UK (33% in 2017), with a reduction of 67% in the period 1998-2017
273 (DEFRA, 2020). This represents a reduction of -3.3 % yr⁻¹ at UK level, which is far from the small street
274 increment trend at Marylebone Road site (-0.2 % yr⁻¹). This large discrepancy could be explained by the
275 use of emission inventories built with EF_{NO_x} that largely underestimate the real emissions in the UK
276 (Carslaw et al., 2011; Carslaw and Rhys-Tyler, 2013) and/or changes in the vehicle fleet composition for
277 certain streets.

278 In relation to the NO₂ concentration trends, both urban background and curbside sites showed long-term
279 improvements, but smaller for the latter where traffic emissions dominate. London presented the smallest
280 decreases in concentration, with slight positive NO₂ street increment but not statistically significant for
281 the study period (1998-2017). The discussion on the NO₂:NO_x emission ratios is further developed in
282 Section 3.2.

283

284 **3.2 Trends in EF for the vehicle fleet**

285 The annual evolutions of the EF_{NO_x} for the vehicle fleet at the three curbside sites over the study period
286 are displayed in Figs. 3a-c. The grey shadows represent the 95% confidence interval of the mean,
287 calculated using the monthly mean values for each year and site. In general, the decreasing trends
288 observed at Jagtvej and Hornsgatan sites for the mixed fleet (Fig. 3 a,c) match the temporal reduction in
289 EF_{NO_x} for different vehicle categories/fuel, as reported by remote sensing studies conducted in European
290 urban areas (Tables 2). These results agree with the introduction of new technologies in the vehicle fleet
291 to reduce air pollution emissions. However, the EF_{NO_x} pattern was rather constant at Marylebone Road
292 over the period (Fig. 3b), and showed a larger monthly variability.

293 Inspecting the normalized Δ NO_x trends (Figs. 3d-f), we can observe a clear resemblance between the
294 EF_{NO_x} trends for Copenhagen and Stockholm (Figs. 3a, c). However, note that the EF_{NO_x} value was
295 reported as the mean of the mixed fleet per vehicle whereas the normalized Δ NO_x does not consider
296 variations in traffic patterns (volume, speed, or vehicle type share). For example, the “bump” observed
297 in the EF_{NO_x} time series at Hornsgatan site in the period 2011-2017 (Fig. 3c) coincided with the reduction
298 in the total TR observed since January 2010, when a ban on studded tires was introduced for the
299 wintertime and which remained over the years (Norman et al., 2016). The normalized Δ NO_x was flat for
300 the same period (Fig. 3f), suggesting that total NO_x emissions might have not changed, but increased per
301 vehicle. We hypothesize that this increase in EF_{NO_x} for the mixed fleet at Hornsgatan site could have

302 been caused by the introduction of buses fueled with 100% Rapeseed Methyl Ester (RME) in 2011, as
303 part of the city of Stockholm's strategy for running the entire bus fleet on renewable fuels and to comply
304 with the Clean Vehicles Directive (2009/33/EC). Note that RME buses emit on average 2.5 times more
305 NO_x than the diesel ones with similar engine and after-treatment technology (Table S2, E5 and Selective
306 Catalytic Reduction SCR). In the year 2011, 10% of the public bus fleet was fueled with 100% RME
307 (Johan Böhlin, personal communication, Feb. 2021), and the RME bus consumption doubled in 2014
308 (Clean Fleets, 2014). This information is consistent with the fast increase in RME sales in the Stockholm
309 county in the period 2011-2017 (Stockholms stad, 2021). The reduction observed in EF_{NO_x} after the year
310 2015 might be mainly associated with the introduction of newer bus engines and/or cleaner exhaust after-
311 treatment technologies for NO_x emissions.

312 The Δ NO_x trend at Marylebone Road demonstrates that, despite all the measures implemented for NO_x
313 control, the total emission remained stable since 2002. According to Font and Fuller (2016), the Δ NO_x
314 trends in London showed a large spatial heterogeneity in the period 2005-2014. They found that
315 increasing Δ NO_x trends were experienced on streets with increasing number of buses per day, such as
316 Marylebone Road in 2010-2014. Conversely, Δ NO_x reductions were associated with a lower traffic
317 volume of buses and/or retrofitted buses with cleaner technologies (such as SCR + Diesel Particulate
318 Filter DPF, Carslaw et al., 2015).

319 The time evolution of the NO₂:NO_x emission ratios for the vehicle fleet is displayed in Figs. 3g-i for the
320 three canyon sites. The interpretation is complex because the mean emission ratio for the whole fleet is
321 influenced by the large variation observed with vehicle category/fuel and Euro standard stage (Tables 2).
322 The fraction of primary NO₂ emissions also depends on the exhaust after-treatment (particularly for
323 buses, Table S2, Supplementary Material), vehicle mileage (Carslaw et al., 2019), mean VS (Grice et al.,
324 2009), ambient temperature (Grange et al., 2019), and engine load (Carslaw et al., 2011; Carslaw and
325 Rhys-Tyler, 2013). Moreover, differences in emission ratios vary considerably from manufacturer to

326 manufacturer even for the same Euro standard stage and model year (Bernard et al., 2018; Carslaw et al.,
327 2019).

328 Grange et al. (2017) showed a clear positive trend in annual mean NO₂:NO_x emission ratios for 61
329 European cities between 1995 and 2010. This trend can be attributed to the wide use of diesel oxidation
330 catalysts (DOC) on PC –that target CO and hydrocarbons, but intentionally convert NO into NO₂ (Fiebig
331 et al., 2014; Russell and Epling, 2011). Remote sensing studies confirm the increase of the NO₂:NO_x
332 emission ratios with the introduction of DOC in E3 diesel PC (Table 2). The overall impact of these
333 primary NO₂ emissions became important due to the dieselization of the European PC fleet, driven by
334 improvements in fuel economy and supposed CO₂ emission reduction (Cames and Helmers, 2013).

335 This dieselization process was strong in the three countries (Figs. 3j-1) with the help of government
336 incentives (Cames and Helmers, 2013). Even though the emission ratios are slightly higher for diesel
337 LCV than for diesel PC for certain Euro stages (Table 2), diesel PC have become abundant at national
338 and urban street levels in more recent times. For example, the shares of diesel PC and LCV in relation to
339 the total fleet on Hornsgatan St. were 33 and 13% in 2017 vs. 17 and 11% in 2009. Note that when the
340 shift towards the use of diesel fuel in PC at the expense of gasoline occurred, increasing NO₂:NO_x
341 emission ratios were clearly observed at Jagtvej and Hornsgatan sites until 2008 and 2010, respectively
342 (Figs. 3g,i). The decay in primary NO₂ emissions observed afterwards might be explained by the
343 development of more efficient DOC systems by the car manufacturers (Carslaw et al., 2016; Carslaw et
344 al., 2019). E6 standards introduced tighter limits for NO_x emissions, and diesel PC were also equipped
345 with NO_x after-treatment systems that increased the NO₂:NO_x emission ratios again (Table 2, E6).

346 Jagtvej and Hornsgatan experienced this increase in emission ratios but differences in time and magnitude
347 might be explained by the composition of the diesel PC fleet per manufacturer group, given the large
348 variations reported by Carslaw et al. (2019). Finally, the absolute NO_x and NO₂ emissions remained low

349 in the period matching the E6 stage, and reductions in ΔNO_x and ΔNO_2 were found at Jagtvej (Figs. 2g,j)
350 and Hornsgatan sites (Figs. 2i,l).

351 Note that certain particular characteristics of the vehicle fleet might arise when analyzing the behavior
352 of $\text{NO}_2:\text{NO}_x$ emission ratios for individual cities and sites. Notably, Marylebone Road showed the
353 maximum peak value (23 vol. %) in 2005 and dropped thereafter (Fig. 3h). This site was largely affected
354 by changes in the urban bus engines and exhaust after-treatment technologies, since the number of buses
355 operating on that street is high (e.g., 1473 buses per weekday in 2003). For example, the steep increase
356 in ratios observed between 2002 and 2003 was attributed to the retrofitting program of London urban
357 buses (E3 stage) with continuously regenerating particle traps (formed by a combination of DOC and
358 DPF, Grange and Carslaw, 2019) and an increase in buses as part of the London congestion charge
359 scheme (Givoni, 2012). The decline in ratios after 2008 was linked to the introduction of buses with
360 newer and cleaner technologies and removal of old buses (Grange and Carslaw, 2019). The peak and
361 decay of $\text{NO}_2:\text{NO}_x$ at Marylebone Road were observed earlier than those in inner London (Carslaw et
362 al., 2016) and we hypothesize that this shift might be due to the different implementation stages in the
363 bus retrofitting programs and bus fleet renewal, depending on the analyzed street. Even though buses
364 largely influence the emissions at Marylebone Road, the contribution of the diesel PC to the emission
365 ratios cannot be ruled out because of their large number (Fig. 3k).

366

367 **3.3 Comparison of EF_{NO_x} at Hornsgatan with literature data**

368 Figure 4 shows the mean EF_{NO_x} for the mixed fleet at Hornsgatan site in the years 2009 and 2017
369 extracted from the EMEP and HBEFA databases, urban remote sensing studies (Table 2), and the results
370 based on inverse modeling. Regardless of the method, lower EF_{NO_x} values were found in 2017 than in
371 2009, following the general trend of decreasing NO_x emissions with the introduction of new engines and
372 after-treatment systems.

373 For both years, the EMEP-based EF_{NO_x} presented the lowest values (0.73 and 0.51 $g\ km^{-1}\ veh^{-1}$ in 2009
374 and 2017, respectively), whereas the results based on HBEFA and remote sensing studies were very
375 similar (1.13 and 1.19 $g\ km^{-1}\ veh^{-1}$ in 2009; 0.92 and 0.98 $g\ km^{-1}\ veh^{-1}$ in 2017). This similarity might be
376 explained by the update of the HBEFA database (V.3.3) with EF_{NO_x} of diesel PC for E4-E6 stages,
377 considering new laboratory and real-world measurements (portable emission monitoring systems and
378 remote sensing data), after compelling evidence that these EF were lower than in-use vehicles studies
379 (Carslaw et al., 2011; Carslaw and Rhys-Tyler, 2013). The EF_{NO_x} presented in the EMEP guidebook
380 were developed with the COPERT model, which has been reported to predict lower NO_x emissions than
381 the HBEFA database under stop-and-go traffic conditions in cities, particularly for diesel vehicles (Borge
382 et al., 2012). A recent UK study (Davison et al., 2021) also found that the national inventory –that heavily
383 relies on the COPERT database– underestimates the NO_x emissions from PC and LCV up to 47% in
384 urban areas compared with emissions calculated with real-world EF_{NO_x} from remote sensing studies.
385 The inverse modeling results presented the highest mean values for both years (1.72 and 1.35 $g\ km^{-1}\ veh^{-1}$
386 ¹ in 2009 and 2017, respectively). The weighted EF_{NO_x} calculations at Hornsgatan street using mean
387 values per vehicle category from remote sensing data (Table 2) was a conservative approach. Considering
388 the upper 95% confidence interval of EF_{NO_x} for each vehicle category yielded weighted EF_{NO_x} values
389 much closer to those obtained with inverse modeling (1.69 and 1.23 $g\ km^{-1}\ veh^{-1}$ in 2009 and 2017,
390 respectively). Moreover, most of the remote sensing studies were conducted in the UK (Table 2), where
391 ambient conditions and the mix of on-road vehicle manufacturers and engine sizes might be different
392 from Hornsgatan St. Thus, all these factors could have contributed to the EF_{NO_x} differences between
393 inverse modeling and remote sensing methods.

394

395 **3.4 Study strengths and limitations**

396 As far as we know, this is the first study to analyze the trends of real-world EF_{NO_x} for the vehicle fleet at
397 the same locations over two decades. Previous studies analyzed NO_x emission trends using only street
398 increment concentrations as a proxy, or remote sensing measurements. Our approach (inverse modeling)
399 presents advantageous features since: (i) we delivered EF_{NO_x} rather than NO_x street increments; this
400 means that we addressed variations in traffic patterns that can largely influence emissions, and (ii) we
401 assessed the overall effectiveness of policies for reducing the fleet emissions over a long time period.
402 Although remote sensing studies provide individual EF_{NO_x} for a large vehicle sample, they might not
403 cover the entire fleet particularly on busy roads with several lanes. Moreover, remote sensing field
404 campaigns are short and traffic and ambient conditions might not be representative of the entire year.
405 This study was limited to the analysis of three paired sites because of the reduced availability of long-
406 term measurements. Hence the transferability of the results to other streets in the same cities should be
407 done cautiously, considering site-specific features and local traffic policies.

408

409 **4. Conclusions**

410 The Euro standard limits for new road vehicles have been successful in reducing NO_x vehicle emissions
411 in the studied sites and the ambient concentrations over time, except for Marylebone Road. This busy
412 street canyon –which experienced an increase in bus traffic since 2003– masked the modest effects of
413 the Euro standard limits on citywide road traffic emissions in London, as shown by the reduction in NO_x
414 concentrations in the urban background atmosphere. The $NO_2:NO_x$ emission ratios showed a positive
415 trend until 2008-2010, which was also reflected in the NO_2 ambient concentrations. This increase was
416 associated with a strong dieselization process and the introduction of new after-treatment technologies
417 that targeted the emission reduction of other species (greenhouse gases, carbon monoxide or particulate
418 matter). Thus, while regulations on ambient concentrations of specific species have positive effects on
419 human health, the overall outcomes should be considered before widely adopting them.

420 Our results suggest revising the low EF_{NOx} values presented in the EMEP guidebook for vehicle
421 emissions, since they are used to compile official national inventories in Europe, estimate the exposures
422 of population to air pollutants and of ecosystems to acidification and eutrophication. Finally, this work
423 showed the relevance of long-term observations combined with dispersion modeling to detect trends, to
424 assess the effectiveness of programs aimed at improving the urban air quality, and to validate emission
425 estimates based on models and laboratory tests.

426

427 **Supplementary Material**

428 Details of air pollution sampling sites, traffic data, meteorological normalization of ambient
429 concentrations, calculation of $NO_2:NOx$ ratios, determination of EF_{NOx} for the mixed fleet, partial
430 dependence plots, and review of real-world EF_{NOx} for urban buses are available.

431

432 **Acknowledgments**

433 We acknowledge Lars Burman (Stockholm Environment and Health Administration) and Johan Böhlin
434 (Stockholm Public Transport, SL) for detailed data and comments on Stockholm traffic emissions. P.
435 Krecl's work was funded by grant 305145/2020-7 from the National Council for Scientific and
436 Technological Development of Brazil (CNPq).

437

438 **References**

439

- 440 Anttila, P., Tuovinen, J.P., 2010. Trends of primary and secondary pollutant concentrations in Finland
441 in 1994-2007. *Atmos. Environ.* 44, 30–41. <https://doi.org/10.1016/j.atmosenv.2009.09.041>
- 442 Atkinson, R.W., Butland, B.K., Anderson, H.R., Maynard, R.L., 2018. Long-term concentrations of
443 nitrogen dioxide and mortality, *Epidemiology*. <https://doi.org/10.1097/EDE.0000000000000847>
- 444 Berkowicz, R., 2000. OSPM: A Parameterised Street Pollution Model. *Environ. Monit. Assess.* 65,
445 323–331.
- 446 Bernard, Y., Tietge, U., German, J., Muncrief, R., Foundation, F.I.A., Transportation, I.C. on C.,
447 NCAP, G., Environment, T. and, Cities, C., 2018. Determination of Real-World Emissions from

448 Passenger Vehicles using Remote Sensing Data 31p.

449 Borge, R., de Miguel, I., de la Paz, D., Lumbreras, J., Pérez, J., Rodríguez, E., 2012. Comparison of
450 road traffic emission models in Madrid (Spain). *Atmos. Environ.* 62, 461–471.
451 <https://doi.org/10.1016/j.atmosenv.2012.08.073>

452 Brown, J.S., 2015. Nitrogen dioxide exposure and airway responsiveness in individuals with asthma.
453 *Inhal. Toxicol.* 27, 1–14. <https://doi.org/10.3109/08958378.2014.979960>

454 Burman, L.; Elmgren, M.; Norman, M., 2019. Fordonsmätningar på Hornsgatan år 2017.

455 Cames, M., Helmers, E., 2013. Critical evaluation of the European diesel car boom - Global
456 comparison, environmental effects and various national strategies. *Environ. Sci. Eur.* 25, 1–22.
457 <https://doi.org/10.1186/2190-4715-25-15>

458 Carslaw, D.C., Beevers, S.D., Tate, J.E., Westmoreland, E.J., Williams, M.L., 2011. Recent evidence
459 concerning higher NO_x emissions from passenger cars and light duty vehicles. *Atmos. Environ.*
460 45, 7053–7063. <https://doi.org/10.1016/j.atmosenv.2011.09.063>

461 Carslaw, D.C., Farren, N.J., Vaughan, A.R., Drysdale, W.S., Young, S., Lee, J.D., 2019. The
462 diminishing importance of nitrogen dioxide emissions from road vehicle exhaust. *Atmos. Environ.*
463 X 1, 100002. <https://doi.org/10.1016/j.aeaoa.2018.100002>

464 Carslaw, D.C., Murrells, T.P., Andersson, J., Keenan, M., 2016. Have vehicle emissions of primary
465 NO₂ peaked? *Faraday Discuss.* 189, 439–454. <https://doi.org/10.1039/c5fd00162e>

466 Carslaw, D.C., Priestman, M., Williams, M.L., Stewart, G.B., Beevers, S.D., 2015. Performance of
467 optimised SCR retrofit buses under urban driving and controlled conditions. *Atmos. Environ.* 105,
468 70–77. <https://doi.org/10.1016/j.atmosenv.2015.01.044>

469 Carslaw, D.C., Rhys-Tyler, G., 2013. New insights from comprehensive on-road measurements of
470 NO_x, NO₂ and NH₃ from vehicle emission remote sensing in London, UK. *Atmos. Environ.* 81,
471 339–347. <https://doi.org/10.1016/j.atmosenv.2013.09.026>

472 Carslaw, D.C., Ropkins, K., 2012. Openair - An R package for air quality data analysis. *Environ.*
473 *Model. Softw.* 27–28, 52–61. <https://doi.org/10.1016/j.envsoft.2011.09.008>

474 Clean Fleets, 2014. Clean Buses – Experiences with Fuel and Technology Options 1–42.

475 Crippa, M., Janssens-Maenhout, G., Dentener, F., Guizzardi, D., Sindelarova, K., Muntean, M., Van
476 Dingenen, R., Granier, C., 2016. Forty years of improvements in European air quality: Regional
477 policy-industry interactions with global impacts. *Atmos. Chem. Phys.* 16, 3825–3841.
478 <https://doi.org/10.5194/acp-16-3825-2016>

479 Davison, J., Rose, R.A., Farren, N.J., Wagner, R.L., Murrells, T.P., Carslaw, D.C., 2021. Verification
480 of a National Emission Inventory and Influence of On-road Vehicle Manufacturer-Level
481 Emissions. *Environ. Sci. Technol.* <https://doi.org/10.1021/acs.est.0c08363>

482 DEFRA. Statistical data set ENV01 - Emissions of air pollutants. Annual update to tables on emissions
483 of important air pollutants in the UK [WWW Document], n.d. URL
484 <https://www.gov.uk/government/statistical-data-sets/env01-emissions-of-air-pollutants> (accessed
485 3.27.21).

486 EEA. European Union emission inventory report 1990-2017. EEA Report. No 08/2019, 2019.

487 Ellermann, T., Nygaard, J., Klenø Nøjgaard, J., Nordstrøm, C., Brandt, J., Christensen, J., Ketzler, M.,
488 Massling, A., Bossi, R., Solvang Jensen, S., 2017. AU Scientific Report from DCE-Danish Centre
489 for Environment and Energy THE DANISH AIR QUALITY MONITORING PROGRAMME
490 Annual Summary for 2017.

491 EMEP/EEA, 2019. Air Pollutant Emission Inventory Guidebook 2019, EEA Report No 13/2019.

492 EN14211. Ambient air — Standard method for the measurement of the concentration of nitrogen
493 dioxide and nitrogen monoxide by chemiluminescence, 2012. . Brussels.

494 EN14625. Ambient air - Standard method for the measurement of the concentration of ozone by
495 ultraviolet photometry. CEN. Brussels, 2012.

496 European Commission. Emissions in the automotive sector [WWW Document], 2021. URL
497 https://ec.europa.eu/growth/sectors/automotive/environment-protection/emissions_en (accessed
498 3.27.21).

499 European Environmental Agency, 2019. European Environmental Agency. Air quality in Europe —
500 2019 report.

501 Fiebig, M., Wiartalla, A., Holderbaum, B., Kiesow, S., 2014. Particulate emissions from diesel engines:
502 Correlation between engine technology and emissions. *J. Occup. Med. Toxicol.* 9, 1–18.
503 <https://doi.org/10.1186/1745-6673-9-6>

504 Font, A., Fuller, G.W., 2016. Did policies to abate atmospheric emissions from traffic have a positive
505 effect in London? *Environ. Pollut.* 218, 463–474. <https://doi.org/10.1016/j.envpol.2016.07.026>

506 Franco, V., Kousoulidou, M., Muntean, M., Ntziachristos, L., Hausberger, S., Dilara, P., 2013. Road
507 vehicle emission factors development: A review. *Atmos. Environ.* 70, 84–97.
508 <https://doi.org/10.1016/j.atmosenv.2013.01.006>

509 Fuzzi, S., Baltensperger, U., Carslaw, K., Decesari, S., Denier Van Der Gon, H., Facchini, M.C.,
510 Fowler, D., Koren, I., Langford, B., Lohmann, U., Nemitz, E., Pandis, S., Riipinen, I., Rudich, Y.,
511 Schaap, M., Slowik, J.G., Spracklen, D. V., Vignati, E., Wild, M., Williams, M., Gilardoni, S.,
512 2015. Particulate matter, air quality and climate: Lessons learned and future needs. *Atmos. Chem.*
513 *Phys.* 15, 8217–8299. <https://doi.org/10.5194/acp-15-8217-2015>

514 Ghaffarpasand, O., Beddows, D.C.S., Ropkins, K., Pope, F.D., 2020. Real-world assessment of vehicle
515 air pollutant emissions subset by vehicle type, fuel and EURO class: New findings from the recent
516 UK EDAR field campaigns, and implications for emissions restricted zones. *Sci. Total Environ.*
517 734, 139416. <https://doi.org/10.1016/j.scitotenv.2020.139416>

518 Givoni, M., 2012. Re-assessing the results of the London congestion charging scheme. *Urban Stud.* 49,
519 1089–1105. <https://doi.org/10.1177/0042098011417017>

520 Grange, S. K.; Farren, N. J.; Vaughan, A. R.; Rose, R. A.; Carslaw, D.C., 2019. Strong temperature
521 dependence for light-duty diesel vehicle NO_x emissions. *Environ. Sci. Technol.* 53, 6587–6596.

522 Grange, S.K., Carslaw, D.C., 2019. Using meteorological normalisation to detect interventions in air
523 quality time series. *Sci. Total Environ.* 653, 578–588.
524 <https://doi.org/10.1016/j.scitotenv.2018.10.344>

525 Grange, S.K., Lewis, A.C., Moller, S.J., Carslaw, D.C., 2017. Lower vehicular primary emissions of
526 NO₂ in Europe than assumed in policy projections. *Nat. Geosci.* 10, 914–918.
527 <https://doi.org/10.1038/s41561-017-0009-0>

528 Grennfelt, P., Engleryd, A., Forsius, M., Hov, Ø., Rodhe, H., Cowling, E., 2020. Acid rain and air
529 pollution: 50 years of progress in environmental science and policy. *Ambio* 49, 849–864.
530 <https://doi.org/10.1007/s13280-019-01244-4>

531 Grice, S., Stedman, J., Kent, A., Hobson, M., Norris, J., Abbott, J., Cooke, S., 2009. Recent trends and
532 projections of primary NO₂ emissions in Europe. *Atmos. Environ.* 43, 2154–2167.
533 <https://doi.org/10.1016/j.atmosenv.2009.01.019>

534 Harrison, R.M., Beddows, D.C.S., Dall’Osto, M., 2011. PMF analysis of wide-range particle size
535 spectra collected on a major highway. *Environ. Sci. Technol.* 45, 5522–5528.
536 <https://doi.org/10.1021/es201998m>

537 International Council on Clean Transportation, 2018. European vehicle market statistics, Pocketbook
538 2018/19 63.

539 Johansson, C., Andersson, C., Bergström, R., Krecl, P., 2008. ITM-rapport 175.

540 Kakosimos, K.E., Hertel, O., Ketzler, M., Berkowicz, R., 2010. Operational Street Pollution Model
541 (OSPM) - A review of performed application and validation studies, and future prospects.
542 *Environ. Chem.* 7, 485–503. <https://doi.org/10.1071/EN10070>

543 Kamińska, J.A., 2019. A random forest partition model for predicting NO₂ concentrations from traffic

544 flow and meteorological conditions. *Sci. Total Environ.* 651, 475–483.
545 <https://doi.org/10.1016/j.scitotenv.2018.09.196>

546 Ketzel, M., Wåhlin, P., Berkowicz, R., Palmgren, F., 2003. Particle and trace gas emission factors
547 under urban driving conditions in Copenhagen based on street and roof-level observations. *Atmos.*
548 *Environ.* 37, 2735–2749. [https://doi.org/10.1016/S1352-2310\(03\)00245-0](https://doi.org/10.1016/S1352-2310(03)00245-0)

549 Keuken, M., Roemer, M., van den Elshout, S., 2009. Trend analysis of urban NO₂ concentrations and
550 the importance of direct NO₂ emissions versus ozone/NO_x equilibrium. *Atmos. Environ.* 43,
551 4780–4783. <https://doi.org/10.1016/j.atmosenv.2008.07.043>

552 Krecl, P., Johansson, C., Targino, A.C., Ström, J., Burman, L., 2017. Trends in black carbon and size-
553 resolved particle number concentrations and vehicle emission factors under real-world conditions.
554 *Atmos. Environ.* 165, 155–168. <https://doi.org/10.1016/j.atmosenv.2017.06.036>

555 Krecl, P., Targino, A.C., Johansson, C., 2011. Spatiotemporal distribution of light-absorbing carbon
556 and its relationship to other atmospheric pollutants in Stockholm. *Atmos. Chem. Phys.* 11, 11553–
557 11567. <https://doi.org/10.5194/acp-11-11553-2011>

558 Krecl, P., Targino, A.C., Johansson, C., Ström, J., 2015. Characterisation and source apportionment of
559 submicron particle number size distributions in a busy street canyon. *Aerosol Air Qual. Res.* 15,
560 220–233. <https://doi.org/10.4209/aaqr.2014.06.0108>

561 Krecl, P., Targino, A.C., Landi, T.P., Ketzel, M., 2018. Determination of black carbon, PM_{2.5}, particle
562 number and NO_x emission factors from roadside measurements and their implications for
563 emission inventory development. *Atmos. Environ.* 186, 229–240.
564 <https://doi.org/10.1016/j.atmosenv.2018.05.042>

565 Laña, I., Del Ser, J., Padró, A., Vélez, M., Casanova-Mateo, C., 2016. The role of local urban traffic
566 and meteorological conditions in air pollution: A data-based case study in Madrid, Spain. *Atmos.*
567 *Environ.* 145, 424–438. <https://doi.org/10.1016/j.atmosenv.2016.09.052>

568 Liefferink, D., Arts, B., Kamstra, J., Ooijevaar, J., 2009. Leaders and laggards in environmental policy:
569 A quantitative analysis of domestic policy outputs. *J. Eur. Public Policy* 16, 677–700.
570 <https://doi.org/10.1080/13501760902983283>

571 Liu, Q., Hallquist, Å.M., Fallgren, H., Jerksjö, M., Jutterström, S., Salberg, H., Hallquist, M., Le
572 Breton, M., Pei, X., Pathak, R.K., Liu, T., Lee, B., Chan, C.K., 2019. Roadside assessment of a
573 modern city bus fleet: Gaseous and particle emissions. *Atmos. Environ.* X 3, 100044.
574 <https://doi.org/10.1016/j.aeaoa.2019.100044>

575 Malley, C.S., Von Schneidemesser, E., Moller, S., Braban, C.F., Kevin Hicks, W., Heal, M.R., 2018.
576 Analysis of the distributions of hourly NO₂ concentrations contributing to annual average NO₂
577 concentrations across the European monitoring network between 2000 and 2014. *Atmos. Chem.*
578 *Phys.* 18, 3563–3587. <https://doi.org/10.5194/acp-18-3563-2018>

579 McDuffie, E.E., Smith, S.J., O'Rourke, P., Tibrewal, K., Venkataraman, C., Marais, E.A., Zheng, B.,
580 Crippa, M., Brauer, M., Martin, R. V., 2020. A global anthropogenic emission inventory of
581 atmospheric pollutants from sector- And fuel-specific sources (1970-2017): An application of the
582 Community Emissions Data System (CEDs). *Earth Syst. Sci. Data* 12, 3413–3442.
583 <https://doi.org/10.5194/essd-12-3413-2020>

584 Monks, P.S., Archibald, A.T., Colette, A., Cooper, O., Coyle, M., Derwent, R., Fowler, D., Granier, C.,
585 Law, K.S., Mills, G.E., Stevenson, D.S., Tarasova, O., Thouret, V., Von Schneidemesser, E.,
586 Sommariva, R., Wild, O., Williams, M.L., 2015. Tropospheric ozone and its precursors from the
587 urban to the global scale from air quality to short-lived climate forcer. *Atmos. Chem. Phys.* 15,
588 8889–8973. <https://doi.org/10.5194/acp-15-8889-2015>

589 Nathan, C., Cunningham-Bussel, A., 2013. Beyond oxidative stress: An immunologist's guide to
590 reactive oxygen species. *Nat. Rev. Immunol.* 13, 349–361. <https://doi.org/10.1038/nri3423>

591 Nielsen, O. -K.; Plejdrup, M. S.; Winther, M.; Mikkelsen, M. H.; Nielsen, M.; Gyldenkerne, S.;

592 Fauser, P.; Albrektsen, R.; Hjelgaard, K. H.; Bruun, H. G.; Thomsen, M., 2019. Annual Danish
593 Informative Inventory Report to UNECE. Emission inventories from the base year of the protocols
594 to year 2017.

595 Norman, M., Sundvor, I., Denby, B.R., Johansson, C., Gustafsson, M., Blomqvist, G., Janhäll, S., 2016.
596 Modelling road dust emission abatement measures using the NORTRIP model: Vehicle speed and
597 studded tyre reduction. *Atmos. Environ.* 134, 96–108.
598 <https://doi.org/10.1016/j.atmosenv.2016.03.035>

599 Olstrup, H., Forsberg, B., Orru, H., Nguyen, H., Molnár, P., Johansson, C., 2018. Trends in air
600 pollutants and health impacts in three Swedish cities over the past three decades. *Atmos. Chem.*
601 *Phys.* 18, 15705–15723. <https://doi.org/10.5194/acp-18-15705-2018>

602 Ottosen, T.B., Kakosimos, K.E., Johansson, C., Hertel, O., Brandt, J., Skov, H., Berkowicz, R.,
603 Ellermann, T., Jensen, S.S., Ketznel, M., 2015. Analysis of the impact of inhomogeneous emissions
604 in the Operational Street Pollution Model (OSPM). *Geosci. Model Dev.* 8, 3231–3245.
605 <https://doi.org/10.5194/gmd-8-3231-2015>

606 Palmgren, F., Berkowicz, R., Ziv, A., Hertel, O., 1999. Actual car fleet emissions estimated from urban
607 air quality measurements and street pollution models. *Sci. Total Environ.* 235, 101–109.
608 [https://doi.org/10.1016/S0048-9697\(99\)00196-5](https://doi.org/10.1016/S0048-9697(99)00196-5)

609 Peel, J.L., Haeuber, R., Garcia, V., Russell, A.G., Neas, L., 2013. Impact of nitrogen and climate
610 change interactions on ambient air pollution and human health. *Biogeochemistry* 114, 121–134.
611 <https://doi.org/10.1007/s10533-012-9782-4>

612 Russell, A., Epling, W.S., 2011. Diesel oxidation catalysts. *Catal. Rev. - Sci. Eng.* 53, 337–423.
613 <https://doi.org/10.1080/01614940.2011.596429>

614 SCB. Emissions of air pollutants from domestic transport by mode of transport. Year 1990 – 2019
615 [WWW Document], 2021. URL
616 https://www.statistikdatabasen.scb.se/pxweb/en/ssd/START__MI__MI0108/MI0108InTransp/
617 (accessed 3.27.21).

618 Snell, J., Birkes, D., Dodge, Y., 1996. *Alternative Methods of Regression*, Wiley Seri. ed, *Journal of*
619 *the Royal Statistical Society. Series A (Statistics in Society)*. Wiley-Interscience.
620 <https://doi.org/10.2307/2983483>

621 Stockholms stad. Proportion of environmental fuel in the Stockholm county [WWW Document], n.d.
622 URL <http://miljobarometern.stockholm.se/miljomal/miljoprogram-2016-2019/miljoanpassade-transporter/minskat-fossilberoende/andel-miljobransle-i-stockholms-lan/rapsbransle/table/>
623 (accessed 3.27.21).

624

625 Swedish Environmental Protection Agency, Informative Inventory Report Sweden 2020, 2020.

626 Transport for London. London Atmospheric Emissions Inventory (LAEI) 2016 [WWW Document],
627 n.d. URL <https://data.london.gov.uk/dataset/london-atmospheric-emissions-inventory--laei--2016>
628 (accessed 3.27.21).

629 Yan, Y., Pozzer, A., Ojha, N., Lin, J., Lelieveld, J., 2018. Analysis of European ozone trends in the
630 period 1995-2014. *Atmos. Chem. Phys.* 18, 5589–5605. <https://doi.org/10.5194/acp-18-5589-2018>

631 Zhou, L., Liu, Q., Lee, B.P., Chan, C.K., Hallquist, Å.M., Sjödin, Å., Jerksjö, M., Salberg, H.,
632 Wängberg, I., Hallquist, M., Salvador, C.M., Gaita, S.M., Mellqvist, J., 2020. A transition of
633 atmospheric emissions of particles and gases from on-road heavy-duty trucks. *Atmos. Chem.*
634 *Phys.* 20, 1701–1722. <https://doi.org/10.5194/acp-20-1701-2020>

635
636
637
638

639 **Tables**

640

641 **Table 1.** Details of the sites and datasets used in this study.

City	Site	Type	Variables	Period
Copenhagen	Jagtvej	Street canyon	NO _x , NO ₂ , TR, VS	1994-2017
	H.C. Ørsted	Urban background	NO _x , NO ₂ , O ₃	
	H.C. Ørsted	Meteorology	T, RH, WS, WD	
London	Marylebone Road	Street canyon	NO _x , NO ₂ , TR, VS	1998-2017
	North Kensington	Urban background	NO _x , NO ₂ , O ₃	
	Heathrow	Meteorology	T, RH, P, WS, WD	
Stockholm	Hornsgatan	Street canyon	NO _x , NO ₂ , TR, VS	1992-2017
	Torkel	Urban background	NO _x , NO ₂ , O ₃	
	Högdalen	Meteorology	T, P, WS, WD	

642 T: air temperature, RH: relative humidity, WS: wind speed, WD: wind direction, P: atmospheric pressure

643

644

645

646

647

648

649

650

651

652

653

654

655

656

657

658

659

660 **Table 2.** Mean EF_{NO_x} and $NO_2:NO_x$ emission ratios for several vehicle categories, taken from remote sensing
661 studies conducted in European cities (UK: Carslaw et al., 2011; Carslaw and Rhys-Tyler, 2013; Carslaw et al.,
662 2019; Ghaffarpasand et al., 2020, and Sweden: Liu et al., 2019; Zhou et al., 2020).

663

Variable	Euro stage	PC gasoline	PC diesel	LCV diesel	Truck (<12 t) diesel	Truck (>12 t) diesel	^a Urban bus diesel
EF_{NO_x} [g km ⁻¹ veh ⁻¹]	E0	2.38	1.22	1.46	5.36	^b n.a.	n.a.
	E1	1.59	1.24	2.27	3.44	n.a.	11.13
	E2	1.05	1.30	2.01	5.95	13.01	12.35
	E3	0.41	1.23	1.83	5.33	10.61	15.58
	E4	0.23	1.00	1.57	5.09	7.75	16.93
	E5	0.14	1.02	1.86	5.33	7.59	12.78
	E6	0.19	0.51	0.67	2.64	0.74	2.40
$NO_2:NO_x$ [vol. %]	E0	3.2	10.8	7.6	6.2	n.a.	n.a.
	E1	2.8	16.8	12.5	11.0	n.a.	11.0
	E2	3.1	8.1	8.4	21.0	11.7	15.4
	E3	4.1	14.9	13.2	12.3	15.8	8.9
	E4	5.6	22.5	23.0	6.2	2.9	8.0
	E5	8.4	18.8	15.5	6.4	4.9	11.3
	E6	10.5	21.7	24.2	15.2	22.5	17.9

664 ^aA large variation could be observed within the same Euro stage, depending on the after-treatment system (Table S2,
665 Supplementary Material). ^bNot available.

666
667
668
669
670
671
672
673
674
675
676
677
678
679
680
681
682
683
684

685 **Figure captions**

686

687 **Figure 1.** Monthly mean NO_x and NO₂ concentrations at curbside and urban background sites (a-f), together with
688 NO_x and NO₂ street increment concentrations (g-l). The orange lines represent the meteorology-normalized
689 concentrations. Note the different y-axis scales adopted to enhance the features in the time series of each site.

690

691 **Figure 2.** Yearly trends (bar plots; in $\mu\text{g m}^{-3} \text{ yr}^{-1}$) and relative changes (numbers; in $\% \text{ yr}^{-1}$) in NO_x (a) and NO₂
692 (b) concentrations for the three cities over the period 1998-2017, based on monthly mean changes in
693 meteorologically normalized air pollutant concentrations at urban background and curbside sites, together with
694 street increments. The error bars show the 95% confidence intervals of the trends. *Indicates that the trend is not
695 significant.

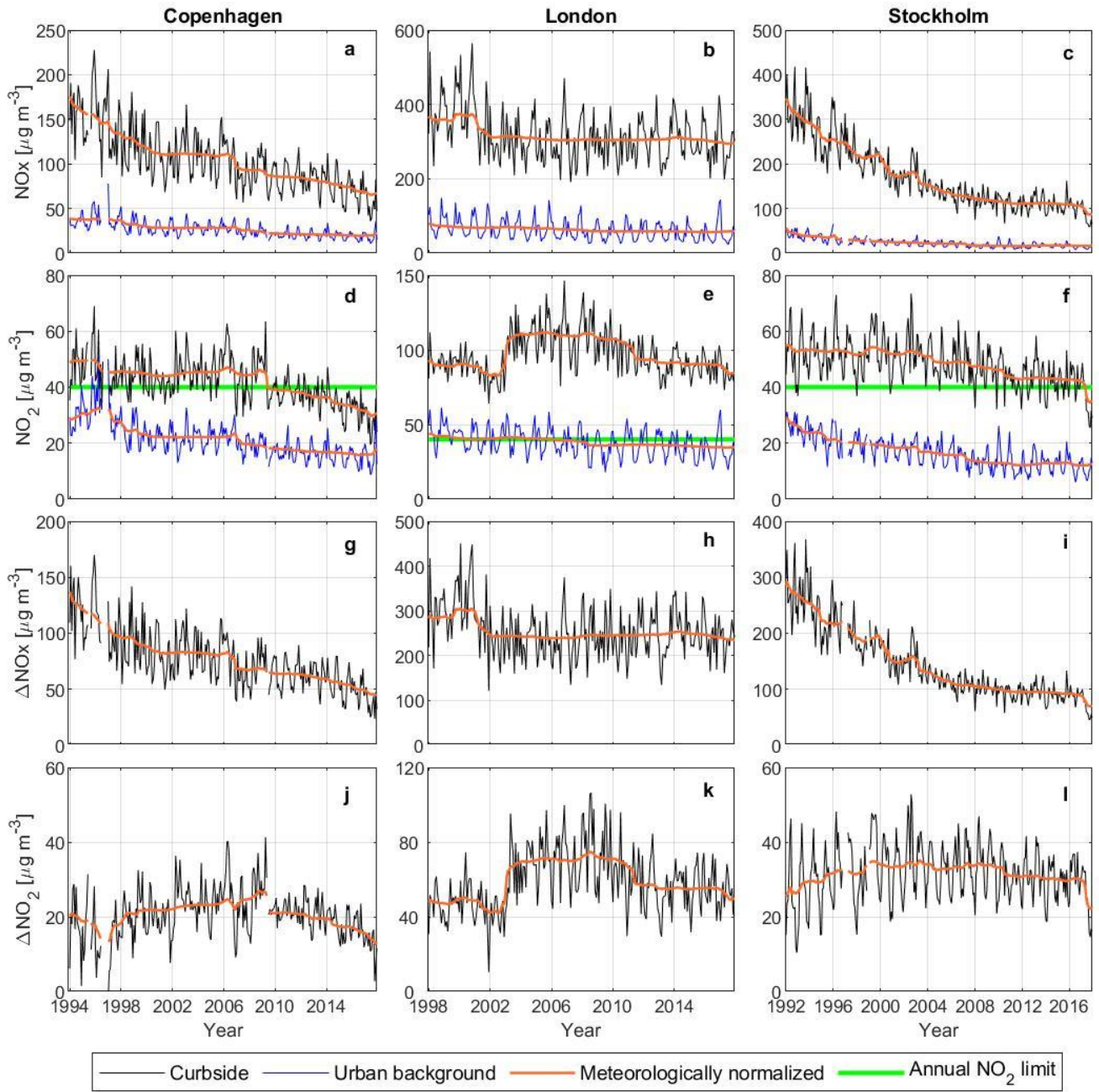
696

697 **Figure 3.** a-c) Annual mean EF_{NO_x} for the vehicle fleet at the curbside sites, with the grey shadows representing
698 the 95% confidence intervals. d-f) Annual mean ΔNO_x concentrations (normalized) at curbside, together with the
699 95% confidence intervals. g-h) Annual NO₂:NO_x emission ratios at curbside with 95% confidence intervals. j-l)
700 Diesel PC penetration in the national markets (International Council on Clean Transportation, 2018) expressed as
701 percentages of all PC (thick black line) and new PC (thin black line), together with Euro standard registration dates
702 (E1: Euro 1, E6: Euro 6).

703

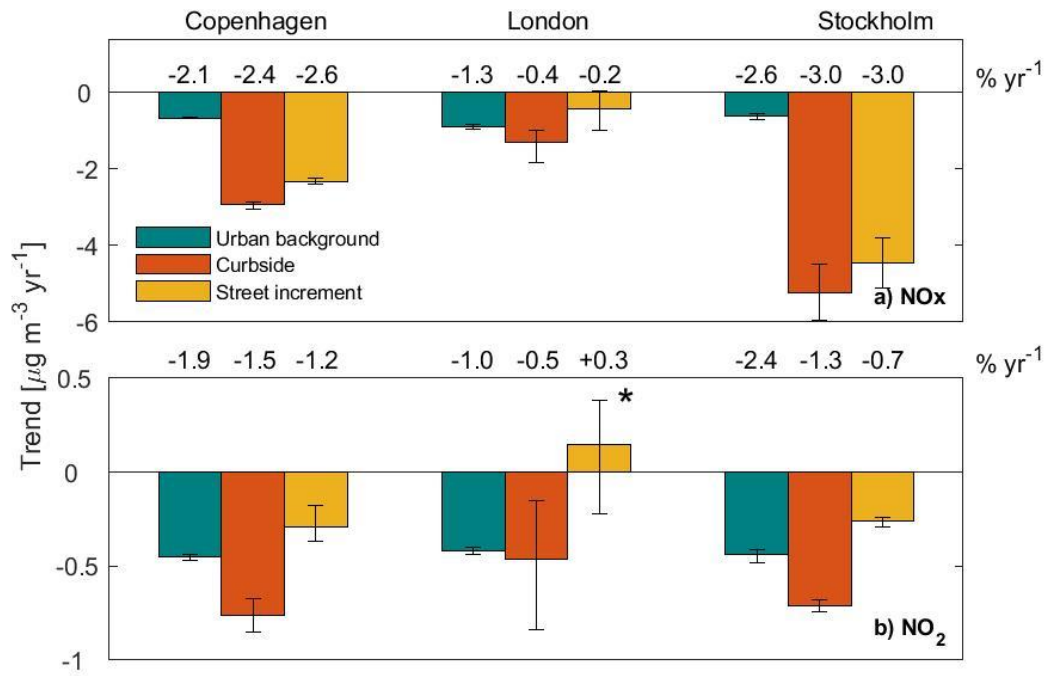
704 **Figure 4.** EF_{NO_x} for the vehicle fleet at Hornsgatan site in the years 2009 and 2017 calculated using databases
705 (EMEP and HBEFA), remote sensing studies (Table 2) and by inverse modeling. The error bars represent the 95%
706 confidence intervals of the mean.

707



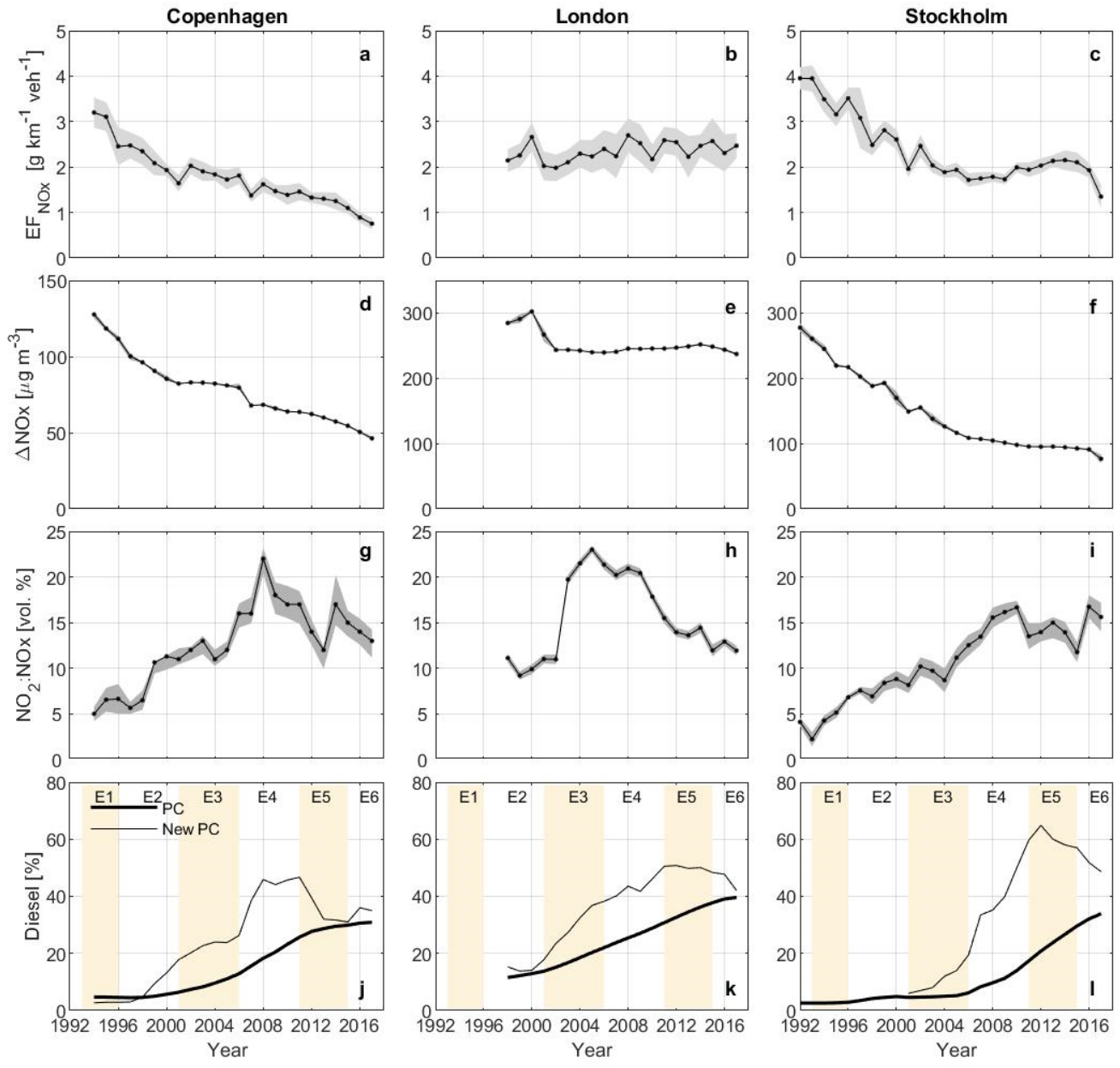
708
709

Figure 1



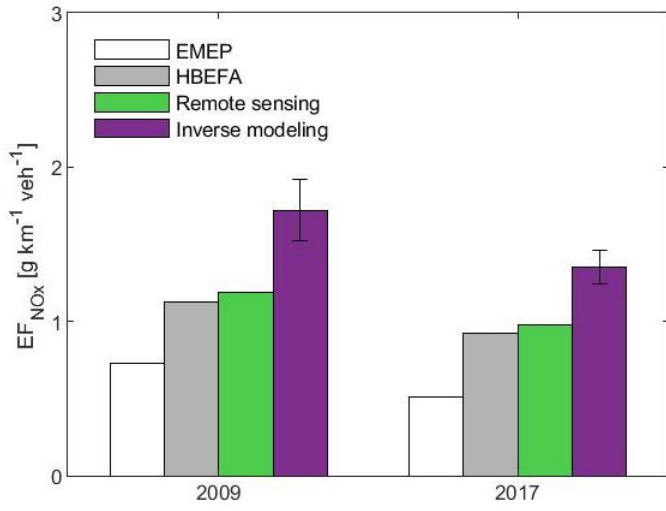
710
711
712

Figure 2



713
714

Figure 3



715
716

Figure 4